see commentary on page 692

The inducible deletion of Drosha and microRNAs in mature podocytes results in a collapsing glomerulopathy

Olga Zhdanova[1,2], Shekhar Srivastava[1,3], Lie Di[1,3], Zhai Li[1], Leila Tchelebi[1], Sara Dworkin[1], Duncan B. Johnstone[4], Jiri Zavadil[5,6], Mark M. Chong[1,7], Dan R. Littman[1,8], Lawrence B. Holzman[4], Laura Barisoni[5] and Edward Y. Skolnik[1,2,3]

[1]The Helen L. and Martin S. Kimmel Center for Biology and Medicine at the Skirball Institute for Biomolecular Medicine, New York University Langone Medical Center, New York, New York, USA; [2]Division of Nephrology, Department of Internal Medicine, New York University Langone Medical Center, New York, New York, USA; [3]Department of Pharmacology, New York University Langone Medical Center, New York, New York, USA; [4]Department of Nephrology, University of Pennsylvania School of Medicine, Philadelphia, Pennsylvania, USA; [5]Department of Pathology, New York University Langone Medical Center, New York, New York, USA; [6]NYU Cancer Institute and Center for Health Informatics and Bioinformatics, New York University Langone Medical Center, New York, New York, USA; [7]The Walter and Eliza Hall Institute of Medical Research, Parkville, Victoria, Australia and [8]Howard Hughes Medical Institute, New York University Langone Medical Center, New York, New York, USA

Micro-RNAs (miRNAs) are short (average 22 nucleotides) noncoding regulatory RNAs that inhibit gene expression by targeting complementary 3′-untranslated regions of protein-encoding mRNAs for translational repression or degradation. miRNAs play key roles in both the function and differentiation of many cell types. Drosha and Dicer, two RNAase III enzymes, function in a stepwise manner to generate a mature miRNA. Previous studies have shown that podocyte-specific deletion of Dicer during development results in proteinuric renal disease and collapsing glomerulopathy (CG); however, Dicer has functions other than the generation of miRNAs. Here we found that the podocyte-specific deletion of Drosha results in a similar phenotype to Dicer mutants, confirming that the Dicer mutant phenotype is due to the loss of miRNAs. Moreover, the inducible deletion of Drosha in 2- to 3-month-old mice (Tet-On system) resulted in CG. Thus, continuous generation of miRNAs are required for the normal function of mature podocytes and their loss leads to CG. Identifying these miRNAs may provide new insight into disease pathogenesis and novel therapeutic targets in various podocytopathies.

Kidney International (2011) **80,** 719–730; doi:10.1038/ki.2011.122; published online 4 May 2011

KEYWORDS: collapsing glomerulopathy; podocyte; proteinuria

Correspondence: *Edward Y. Skolnik, Division of Nephrology, Department of Internal Medicine, New York University Langone Medical Center, New York, New York 10016, USA. E-mail: Edward.Skolnik@nyumc.org*

Received 13 October 2009; revised 4 March 2011; accepted 15 March 2011; published online 4 May 2011

Micro-RNAs (miRNAs) are short (~22 nucleotides) non-coding regulatory RNAs in plants and animals that inhibit gene expression by targeting protein-encoding mRNAs for translational repression or degradation.[1,2] MiRNAs bind to complementary sites within the 3′-untranslated regions of their target mRNAs.[3,4] The generation of miRNAs starts from transcription of large RNA precursors, termed pri-miRNAs, from the genome by RNA polymerase II or III. Pri-miRNAs are then processed in the nucleus into shorter sequences of ~70 nucleotides, termed pre-miRNAs, by the RNase III enzyme Drosha and the protein Pasha complex.[5–7] Pre-miRNAs have imperfect stem-loop structure and are transported into the cytoplasm where the RNase III enzyme, Dicer, and its double-stranded RNA binding partner, the human immunodeficiency virus-1 transactivating response RNA-binding protein, excise double-stranded miRNAs of ~22 nucleotides.[8,9] The miRNA joins the miRISC (miRNA-associated multiprotein RNA-induced silencing complex).[10] The mature miRNA strand is preferentially retained in the miRISC and guides it to the target sequence.

At present, over 1000 miRNAs have been identified in humans/mammals. Current estimates predict that ~60% of all human genes are regulated by miRNAs,[11] with a single miRNA capable of binding and regulating >200 target sequences. A large number of papers have now described the functional roles for miRNAs in a number of biological processes including cell fate and differentiation, development, cell proliferation, and apoptosis.[12–14] It is also evident that miRNAs play critical roles in maintaining normal health and tissue homeostasis, and changes in miRNA expression are highly relevant to disease processes.

Recently, a number of studies have begun to address the role of miRNAs in kidney disease.[15] These studies have

demonstrated that a number of miRNAs are expressed in the kidney, and changes in miRNA expression may contribute to disease.[16,17] Targeted deletion of Dicer in proximal tubule cells has been shown to protect mice from ischemic reperfusion injury.[18] In diabetic nephropathy, transforming growth factor-β upregulation of miR-216a and miR-217 in mesangial cells may promote their survival and hypertrophy, whereas upregulation of miR-377 by high glucose may contribute to mesangial cell production of fibronectin,[19] and downregulation of miR192 in proximal tubule cells may contribute to interstitial fibrosis.[19,20] Changes in miRNA expression patterns may also contribute to hepatic and renal cyst formation in autosomal dominant polycystic kidney disease,[21,22] and may serve as biomarkers for kidney transplant rejection.[23]

In addition to the above studies, three reports have recently shown that miRNAs may also play critical roles in podocyte homeostasis.[24–26] These studies demonstrated that podocyte-specific deletion of Dicer led to podocyte dysregulation, resulting in proteinuric renal disease and collapsing glomerulopathy (CG) with glomerular and tubulointerstitial fibrosis and renal failure at ~6–8 weeks of age. However, in addition to playing a critical role in miRNA biogenesis, Dicer also has functions that are independent of miRNA biogenesis. For example, Dicer is also critical for generating small inhibitory RNAs derived from endogenous or exogenous double-stranded RNA transcripts.[27,28] Thus, although decreased expression of miRNAs in podocytes lacking Dicer has been implicated in the development of the CG phenotype, it is not known whether this phenotype is due solely to the loss of miRNAs or whether miRNA-independent functions of Dicer contribute to the phenotype. Moreover, as Dicer is deleted in developing kidneys in these studies, it still remains to be determined whether the inducible deletion of dicer in a fully developed kidney also results in a similar phenotype.

To address whether the phenotype in podocyte-specific Dicer knockouts (KOs) is due solely to miRNA-dependent regulation of normal podocyte function, or whether other functions of Dicer contribute to the phenotype observed, we generated mice in which Drosha was specifically deleted in podocytes. We found that specifically inactivating Drosha in podocytes led to CG that was comparable with the podocyte-specific Dicer KOs previously described. In addition, we found that inducibly deleting Drosha in podocytes at 2 months of age also led to a CG. Thus, these findings reinforce the critical role for miRNAs in normal podocyte biology and suggest that identifying changes in miRNA expression in various podocyte diseases may provide novel therapeutic targets to treat disease.

RESULTS

Podocyte-specific deletion of Drosha results in CG that is comparable with Dicer KOs

Drosha$^{fl/fl}$ mice have been previously described,[29] in which exon 9 is flanked by *loxP* sites. Deletion of exon 9 disrupts both the full-length Drosha and two alternately spliced forms and results in a frameshift and the appearance of multiple stop codons. Podocyte-specific Drosha KO mice were generated by breeding *Drosha*$^{fl/fl}$ to *NPHS2-Cre; Drosha*$^{fl/+}$ (NPHS2-Cre mice were provided by L Holzman, University of Michigan). *Dicer*$^{fl/fl}$ mice were provided by M McManus (University of California, San Francisco, CA) and have been previously described.[30] Podocyte-specific Dicer KOs were generated by crossing *Dicer*$^{fl/fl}$ to *NPHS2-Cre; Dicer*$^{fl/+}$.

NPHS2-Cre; Drosha$^{fl/fl}$ mice were born at the expected Mendelian frequency. However, *NPHS2-Cre; Drosha*$^{fl/fl}$ mice developed proteinuria at about ~2 to 3 weeks of age that progressed overtime with renal failure and death occurring between 4 and 8 weeks of age (Figure 1 and data not shown). *NPHS2-Cre; Drosha*$^{fl/+}$ mice containing a heterozygous deletion of Drosha in podocytes were phenotypically normal and did not develop proteinuria or histological evidence of kidney disease up until 12 months of age.

Histological examination of *NPHS2-Cre; Drosha*$^{fl/fl}$ mice until postnatal day 14 revealed normal glomeruli with no apparent abnormality in glomerular development by either light or electron microscopy (data not shown). However, significant glomerular pathology became apparent after postnatal day 14 that progressed over time. At 3 weeks of age, kidneys from *NPHS2-Cre; Drosha*$^{fl/fl}$ mice were smaller and paler when compared with *NPHS2-Cre; Drosha*$^{+/+}$ kidneys. Extensive foot process effacement and mild wrinkling of the glomerular basement membranes on electron microscopy was the earliest pathologic finding and coincided with the onset of proteinuria (Figure 2b, early). Histopathological examination of *NPHS2-Cre; Drosha*$^{fl/fl}$ kidneys by periodic acid-Schiff stain between 2 and 3 weeks of age revealed only very focal collapsing changes (affecting ~10% of the total number of glomeruli), and rare (0.5–1+) cystic dilatation of tubules as well as microcysts, which contained protein casts in the lumen.

At 4–6 weeks of age, kidneys from *NPHS2-Cre; Drosha*$^{fl/fl}$ mice demonstrated extensive CG, with extensive segmental and/or global collapse of the glomerular tuft coupled with marked extracapillary proliferation (Figure 2a and Tables 1 and 2). Pseudocrescent formation was found in ~45% of glomeruli and segmental or global sclerosis was seen in 28% of the total number of glomeruli, indicating progression of the disease. Simultaneously, the remaining parenchyma was also remarkable for extensive microcyst formation (3+) (Figure 2a and Tables 1 and 2). On ultrastructural analysis, collapsing features were more severe and complete occlusion of the glomerular capillary lumina by severe collapse of the glomerular basement membranes could be appreciated, together with extensive podocyte injury with the loss of primary and secondary foot processes (Figure 2b, advanced). These changes were proportional to the extent and duration of proteinuria. Similar pathology was found in kidneys from *NPHS2-Cre; Dicer*$^{fl/fl}$ mice (Tables 1 and 2 and Figure 2a and b), although kidneys from *NPHS2-Cre; Drosha*$^{fl/fl}$ mice exhibited more severe disease at younger age (data not shown).

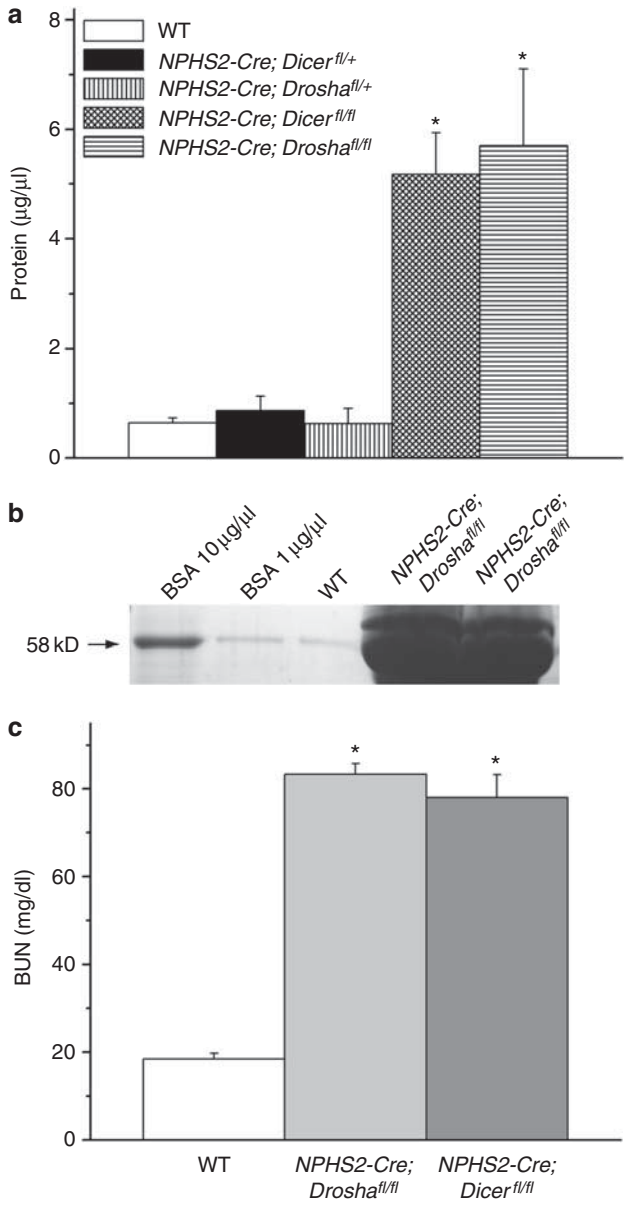

Figure 1 | *NPHS2-Cre; Drosha$^{fl/fl}$* develop proteinuria and renal failure. (**a**) Protein concentration in urine obtained from wild-type (WT; *NPHS2-Cre; Drosha$^{+/+}$*), heterozygous (*NPHS2-Cre; Drosha$^{fl/+}$*), and homozygous Drosha (*NPHS2-Cre; Drosha$^{fl/fl}$*), and Dicer (*NPHS2-Cre; Dicer$^{fl/fl}$*) mutants determined by Bradford assay ($n = 5$ mice in each group). Differences in protein concentrations were statistically significant for homozygous Drosha and Dicer mice when compared with WT and homozygous animals (*$P < 0.05$). (**b**) From 4-week-old WT and homozygous Drosha mutants, 10 µl of urine was separated by sodium dodecyl sulfate (SDS)-polyacrylamide gel electrophoreses (10%) followed by Coomassie staining. Bovine serum albumin (BSA) was run as a control. (**c**) Blood urea nitrogen (BUN) concentration was determined in 4-week-old WT and homozygous Drosha and Dicer mutants ($n = 5$ mice in each group). BUN values were statistically significant in homozygous Drosha and Dicer mice when compared with WT mice (*$P < 0.05$).

Deletion of Drosha in podocytes leads to podocyte dedifferentiation and loss of the podocyte-specific markers synaptopodin, Wilms' tumor-1 (WT-1), podocin, and nephrin

CG is associated with podocyte dedifferentiation and loss of podocyte-specific markers. Podocytes from *NPHS2-Cre; Drosha$^{fl/fl}$* mice exhibited loss of synaptopodin and WT-1, which was first noted at the onset of proteinuria and progressed over time as the kidney disease progressed (Figure 3 and Table 3). Similar findings were found in kidneys from *NPHS2-Cre; Dicer$^{fl/fl}$* mice (Figure 3 and Table 3), with the exception that WT-1 expression was lost at an earlier age in *NPHS2-Cre; Drosha$^{fl/fl}$* mice, which is consistent with kidneys from *NPHS2-Cre; Drosha$^{fl/fl}$* mice exhibiting a more severe phenotype at an earlier age (data not shown).

Podocin and nephrin expression were examined by immunofluorescent staining in *NPHS2-Cre; Drosha$^{fl/fl}$* mice of different ages to further characterize the temporal course of podocyte injury. The glomeruli of *NPHS2-Cre; Drosha$^{fl/fl}$* mice with minimal changes of CG (age 2 weeks) showed near-normal levels of nephrin and podocin expression when compared with wild-type animals (Figure 4a and b), indicating that podocyte development is normal in *NPHS2-Cre; Drosha$^{fl/fl}$* mice. However, at 5–6 weeks of age when *NPHS2-Cre; Drosha$^{fl/fl}$* mice have severe CG, levels of both nephrin and podocin were significantly reduced in glomeruli of *NPHS2-Cre; Drosha$^{fl/fl}$* mice. Nephrin and podocin also displayed a disorganized and granular pattern of distribution in *NPHS2-Cre; Drosha$^{fl/fl}$* mice that could also be appreciated in glomeruli with early podocyte injury (Figure 4a and b).

Deletion of Drosha in podocytes leads to increased podocyte proliferation and apoptosis and upregulation of desmin and smooth muscle actin (SMA)

Tissue injury in a number of different cell types is frequently associated with increased expression of intermediate filament proteins.[31] In podocytes, the intermediate filament protein desmin is upregulated in a number of experimental models of podocyte injury.[32–34] Desmin is also upregulated in glomeruli in *NPHS2-Cre; Drosha$^{fl/fl}$* mice, which is consistent with significant podocyte damage in these mice. Desmin-positive cells were primarily localized to proliferating cells (Ki-67 positive) in the urinary space, which were likely podocytes because they also stained for the podocyte-specific marker nestin[35] (Figure 5 and Table 3). Quantification of podocyte proliferation in *NPHS2-Cre; Drosha$^{fl/fl}$* mice demonstrated an increase in the proliferative index (PI) in epithelial cells in the urinary space (Table 4, PI in *NPHS2-Cre; Drosha$^{fl/fl}$* mice (4–6 weeks) = 0.656 (range 0.261–0.753); PI in *NPHS2-Cre; Drosha$^{fl/fl}$* mice (2 weeks) = 0; PI in *NPHS2-Cre; Drosha$^{+/+}$* mice = 0). In addition, SMA was also upregulated in glomeruli of *NPHS2-Cre; Drosha$^{fl/fl}$* mice (Figure 5a). Although early on in disease SMA is most prominently localized periglomerularly (data not shown), in advanced disease cells in the urinary space stained prominently for SMA (Figure 5a). Podocytes from *NPHS2-Cre; Drosha$^{fl/fl}$* also

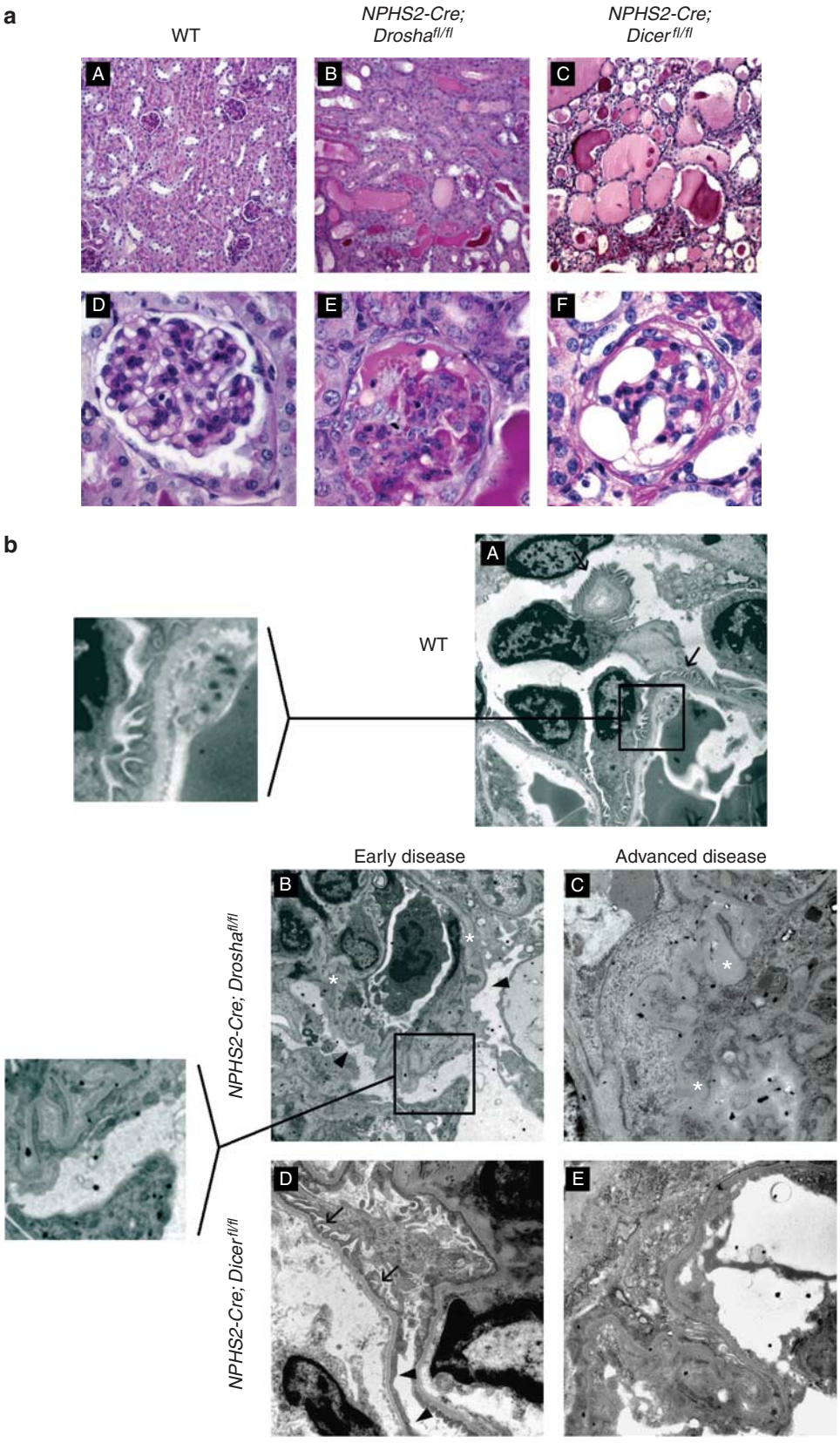
a
WT
NPHS2-Cre; Drosha fl/fl
NPHS2-Cre; Dicer fl/fl
A
B
C
D
E
F
b
WT
A
Early disease
Advanced disease
NPHS2-Cre; Drosha fl/fl
B
C
NPHS2-Cre; Dicer fl/fl
D
E

Table 1 | Histological analysis between 4 and 6 weeks of age

Genotype/phenotype	% Segm sclerosis	% Segm collapse	% Global sclerosis	% Global collapse	Tubular microcysts
NPHS2-Cre; Drosha$^{+/+}$	0	0	0	0	0
NPHS2-Cre; Drosha$^{fl/fl}$	14.5	14.8	12.7	29.9	3+
NPHS2-Cre; Dicer$^{fl/fl}$	9.3	14.8	26.3	22.9	3+

Global collapse: global wrinkling and folding of the glomerular basement membranes with hypertrophy and hyperplasia of overlying podocytes filling the urinary space; Global sclerosis: global solidification of tuft; Segmental collapse: segmental wrinkling and folding of the glomerular basement membranes with hypertrophy and hyperplasia of overlying podocytes; Segmental sclerosis: segmental solidification of the glomerular tuft with adhesion to the Bowman's capsule; Tubular microcysts: defined as dilated tubules containing hyaline casts. The amount of microcysts is calculated on a semiquantitative scale from 0 to 3+ (0=no cysts; ±=<10 cysts total at ×40; 1+=1–3 cysts in at least 5 fields at ×40; 2+=4–10 cysts in at least 5 fields at ×40; 3+=>11 cysts in at least 5 fields at ×40).

Table 2 | Characterization of renal disease in *NPHS2-Cre; Drosha*$^{fl/fl}$ and *NPHS2-Cre; Dicer*$^{fl/fl}$ mice

	NPHS2-Cre; Drosha$^{+/+}$	*NPHS2-Cre; Drosha*$^{fl/fl}$	*NPHS2-Cre; Dicer*$^{fl/fl}$
Proteinuria	–	+++	+++
Glomerular sclerosis and collapse[a]	0%	71.9%	73.4%
Tubular microcysts[a]	0	3+	3+
Podocyte phenotype[b]	Normal	Abnormal	Abnormal
Foot process effacement	0%	100%	100%
Primary processes	Present	Absent	Absent

[a]See Table 1 legend for details.
[b]Details of podocyte phenotype with regard to podocin, nephrin, synaptopodin, Wilms' tumor, ki-67, smooth-muscle actin, desmin, and nestin are discussed in the text and shown in Figures 3, 4, 5 and Table 3.

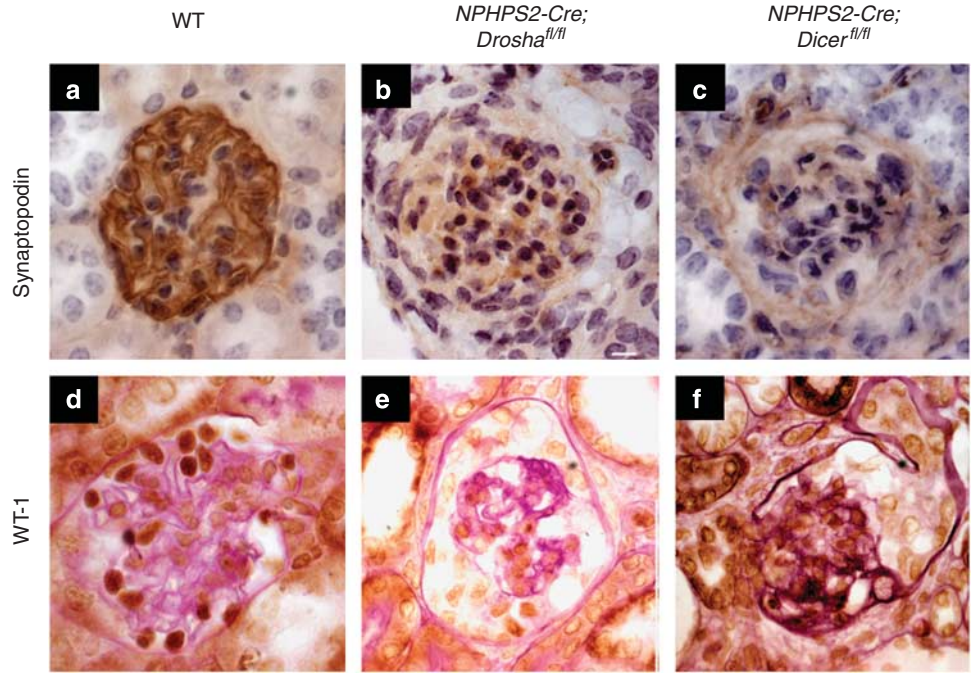

Figure 3 | Podocytes from Drosha and Dicer mutants have decreased expression of synaptopodin and Wilms' tumor-1 (WT-1). Immunohistochemistry of histological sections from 4- to 5-week-old wild-type (WT), Drosha, and Dicer mutants immunostained with antibodies to synaptopodin and WT-1. Podocyte expression of synaptopodin and WT-1 are decreased in both Drosha and Dicer mutants.

Figure 2 | *NPHS2-Cre; Drosha*$^{fl/fl}$ develop collapsing glomerulopathy with focal glomerulosclerosis with pseudocrescents and microcystic dilatation of tubules. (**a**) Histological examination (periodic acid-Schiff (PAS) stain) of kidneys from wild-type (WT; *NPHS2-Cre; Drosha*$^{+/+}$) and homozygous Drosha (*NPHS2-Cre; Drosha*$^{fl/fl}$) and Dicer (*NPHS2-Cre; Dicer*$^{fl/fl}$) mutants at 4 to 5 weeks of age. Upper panel, original magnification ×20 (A–C); lower panel, original magnification ×40 (D–F). (**b**) Electron microscopy of kidneys from WT (A) or homozygous Drosha and Dicer mutants at 2 weeks (early disease B, D) or 4 to 5 weeks (advanced disease C, E) of age. Arrows indicate normal podocyte foot processes. Arrowheads indicate effaced podocyte foot processes. Asterisks indicate collapsed glomerular basement membrane. Insert in panel A shows normal podocyte foot processes. Insert in panel B shows effaced podocyte foot processes.

Table 3 | Podocyte phenotype—immunohistochemical analysis

	NPHS2-Cre; Drosha$^{+/+}$	*NPHS2-Cre; Drosha$^{fl/fl}$*	*NPHS2-Cre; Dicer$^{fl/fl}$*
Synaptopodin	+	−	−
WT-1	+	−	−
Nestin	+	+	+
SMA	−	+	+
Desmin	−	+	+
Ki-67	−	+	+

Abbreviations: −, Negative staining; +, positive staining; SMA, smooth muscle actin; WT-1, Wilms' tumor-1.

exhibited increased apoptosis compared with wild-type animals and the increase in apoptosis increased with time as CG became more advanced (Figure 5b).

Conditional inducible deletion of Drosha in podocytes at 2 months of age also results in a CG

In order to determine whether miRNAs are required for the normal function of mature podocytes, a Tet-On system was utilized to specifically delete Drosha in podocytes in 2-month-old animals. *Drosha$^{fl/fl}$; podocin-rtTA$^{Tg/+}$; tetO-Cre$^{Tg/+}$* mice were either administered or not administered doxycycline at 2 months of age and kidneys were analyzed 1 month later. Previous studies have demonstrated specific deletion of the gene of interest in 80% of podocytes in these mice using a Z/EG reporter.[36] We have also confirmed specific deletion of exon 9 of the *Drosha* gene in glomeruli isolated only from mice given doxycycline (Figure 6a). As expected, kidneys sections were normal in animals not exposed to doxycycline (Figure 6c, A and C), and these mice did not develop proteinuria (Figure 6b). In contrast, *Drosha$^{fl/fl}$; podocin-rtTA$^{Tg/+}$; tetO-Cre$^{Tg/+}$* mice administered doxycycline developed proteinuria beginning ~2 weeks after starting doxycycline (Figure 6b), which on histological examination revealed a phenotype that was very similar to the phenotype observed in the conditional KOs shown in Figure 2. Kidneys from mice administered doxycycline for 1 month had numerous tubular microcysts accompanied by a dense interstitial inflammation (Figure 6b, B), which on higher magnification revealed shrunken glomeruli, with collapsed capillary walls and proliferation of epithelial cells that filled the urinary space (Figure 6b, D). Thus, these results demonstrate that miRNAs are required for the maintenance of normal podocyte function and suggest that primary changes in specific miRNAs may contribute to disease.

In order to begin to identify candidate miRNAs that are critical for normal podocyte function, glomeruli were isolated by laser capture microscopy from *Drosha$^{fl/fl}$; podocin-rtTA$^{Tg/+}$; tetO-Cre$^{Tg/+}$* and *Drosha$^{fl/+}$; podocin-rtTA$^{Tg/+}$; tetO-Cre$^{Tg/+}$* 4 weeks following administration of doxycycline, and miRNA expression was quantitated by Taqman low density micro arrays (Applied Biosystems by Life Technologies, Carlsbad, CA). These experiments identified 10 miRNAs that were consistently undetectable in mice in which Drosha was conditionally inducibly deleted in podocytes when compared with heterozygote animals (Figure 7).

DISCUSSION

In this study we demonstrate that conditional deletion of Drosha in podocytes results in CG that is similar to three previous reports that studied mice with a conditional deletion of Dicer in podocytes.[24–26] Although both Drosha and Dicer have been shown to function in series to generate a mature miRNA, both RNAase molecules have distinct functions. For example, it is now appreciated that Dicer also plays a role in processing pseudogene-derived double-stranded RNAs into small inhibitory RNAs in mammals.[27,28,37] Thus, it remained a possibility that the kidney phenotype in podocyte-specific Dicer KOs was contributed by other functions of Dicer. Moreover, whether Dicer and by extension miRNAs are critical for function of fully differentiated mature podocytes was not addressed in these previous studies. Our findings reported here when taken together reinforce the importance for miRNAs in podocyte homeostasis and/or development, and demonstrate for the first time that mature podocytes require the continued expression of miRNAs for normal function.

Conditional deletion of Drosha in podocytes resulted in a kidney lesion with many of the hallmarks of CG.[38,39] The earliest phenotype observed was foot process effacement on electron microscopy, which was accompanied by proteinuria. As the disease progressed, podocytes underwent dedifferentiation, leading to the loss of expression of podocyte-specific genes such as podocin, nephrin, synaptopodin, and WT-1. These changes were accompanied by glomerular tuft collapse, wrinkling of the basement membrane, and pseudocrescent formation, which ultimately led to renal failure and death in most mice by 6 weeks of age.

One of the hallmarks of CG is the accumulation of proliferating epithelial cells in Bowman's space.[38–41] This is in contrast to other podocyte diseases, such as focal segmental glomerular sclerosis, which is associated with podocyte loss and lack the proliferative component seen in CG. Consistent with the histological features of CG, *NPHS2-Cre; Drosha$^{fl/fl}$* mice also had marked epithelial cell proliferation in glomeruli as assessed by Ki-67 staining. One of the controversies has been whether the proliferating cells in CG derive from dedifferentiated podocytes or the parietal epithelial cells that line the urinary space.[42–46] Lineage-tracing experiments have provided support for the contribution of both cell types to the proliferating epithelial cells in Bowman's space, depending upon the model studied.[42,43,46,47] Our finding that ~80% of the proliferating epithelial cells in *NPHS2-Cre; Drosha$^{fl/fl}$* mice express the podocyte-specific marker nestin as well as desmin suggests that the majority of cells in the urinary space that form pseudocrescents are podocytes in origin. This would be in agreement with the podocyte lineage-tracing experiments by Moeller *et al.*[45,47] as well as studies by Thorner *et al.*[35] While the mechanism whereby podocyte injury predisposes to the formation of

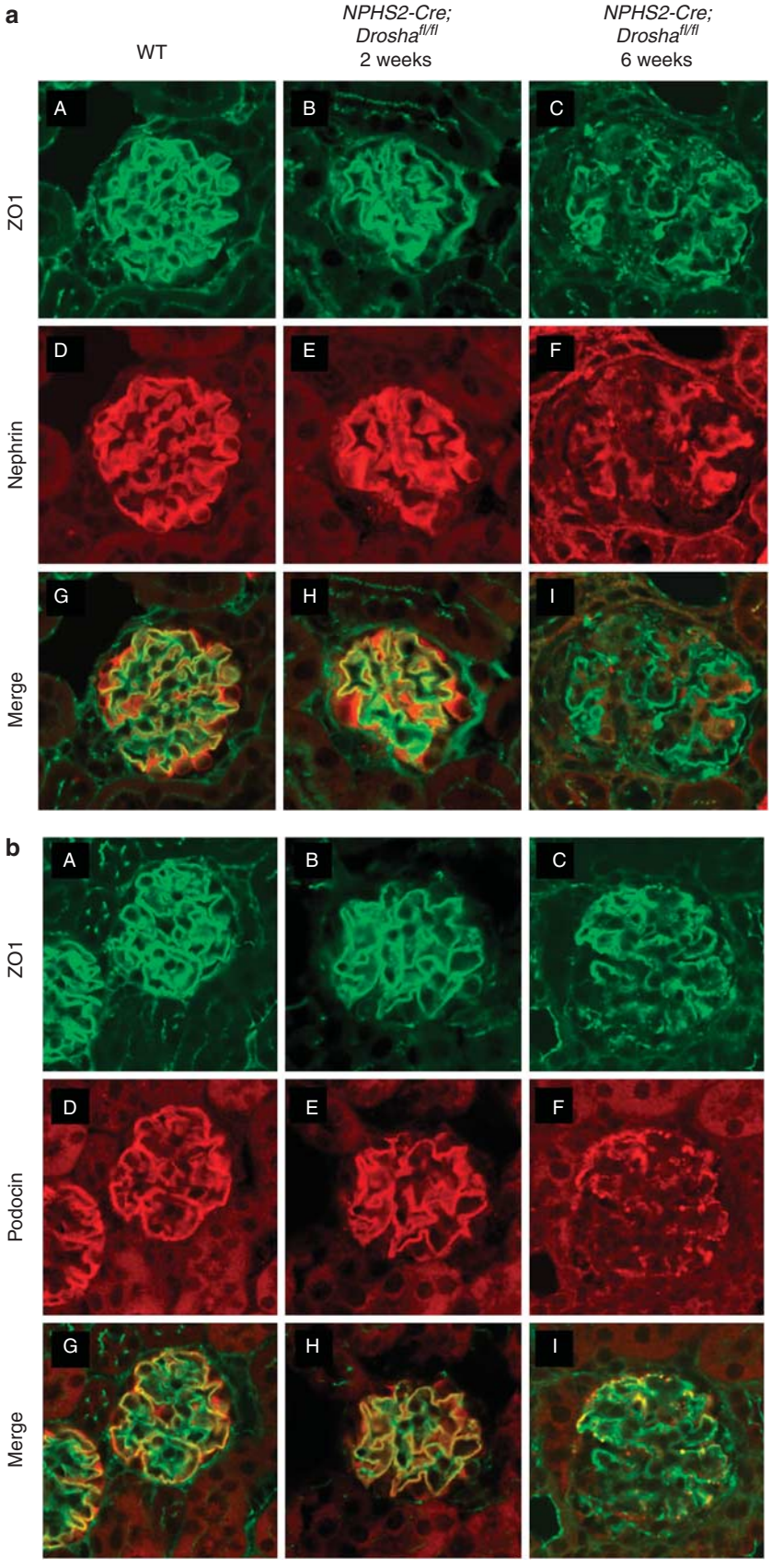

Figure 4 | Expression of podocin and nephrin in wild-type (WT) and Drosha mutants. Immunofluorescence of histological sections from WT and Drosha mutants at 2 and 6 weeks of age stained with antibodies to (**a**) nephrin (D–F) and (**b**) podocin (D–F). Sections were also stained with anti-ZO1 to mark adherent junctions on podocytes (**a**) A–C and (**b**) A–C and ZO–1 colocalization with nephrin (**a**) G–I and podocin (**b**) G–I.

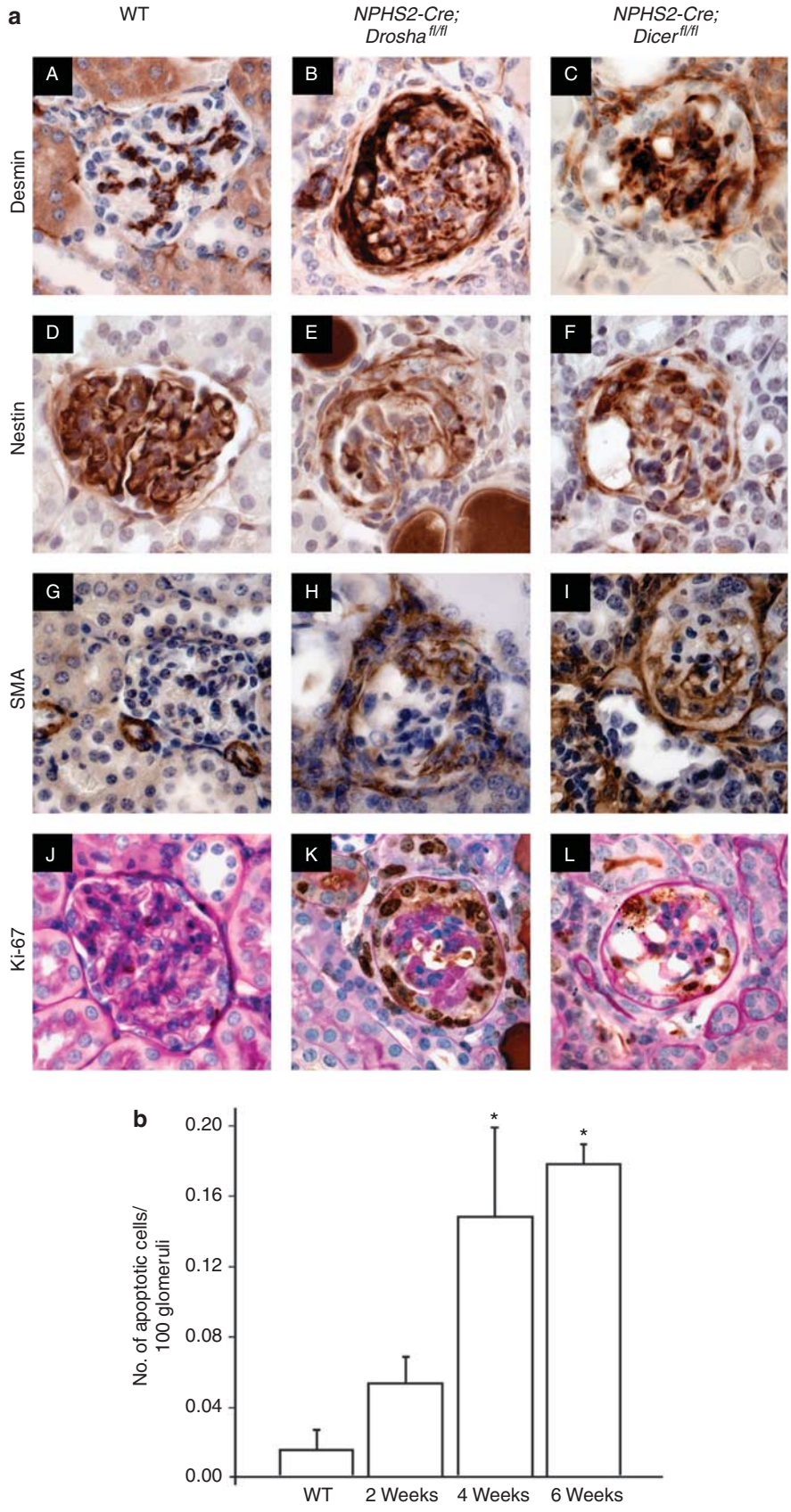
a
WT
NPHS2-Cre; Drosha fl/fl
NPHS2-Cre; Dicer fl/fl
Desmin
Nestin
SMA
Ki-67
A
B
C
D
E
F
G
H
I
J
K
L
b
No. of apoptotic cells/ 100 glomeruli
0.20
0.16
0.12
0.08
0.04
0.00
*
*
WT
2 Weeks
4 Weeks
6 Weeks

pseudocrescents derived predominantly from podocytes or parietal epithelial cells is still unknown, these findings raise the possibility that specific miRNAs in podocytes are critical to maintaining podocytes in a nonproliferative differentiated state. Thus, loss of specific miRNAs in some diseases that affect podocytes may be one of the factors that determine whether podocytes are able to undergo a phenotypic switch that allows them to contribute to pseudocrescent formation. This is consistent with the known functions of miRNAs in other cell types. For example, it has been shown that miR-1 and miR-206 play critical roles in skeletal muscle differentiation by maintaining skeletal muscle in a quiescent state.[48,49]

Epithelial cells derived from *NPHS2-Cre; Drosha*$^{fl/fl}$ mice express the intermediate filament desmin and α-SMA. Although desmin has been shown to be upregulated in damaged podocytes,[33,34] our finding that desmin-positive cells in *NPHS2-Cre; Drosha*$^{fl/fl}$ mice also express SMA raises the possibility that these cells are undergoing a type 2 epithelial-mesenchymal transition (EMT),[50,51] which contributes to glomerular fibrosis and renal failure. EMT is not an easy diagnosis to make *in vivo*, as currently there is not a single specific change that marks this transition. Rather, it has now been proposed that analyzing changes in expression of a number of different markers, including cytoskelatal proteins, transcription factors, matrix proteins, cell surface receptors, and miRNAs, are required to identify cells undergoing EMT.[50] So far, we have been unable to demonstrate expression of some other markers of EMT in these cells, such as snail and β-catenin. Nevertheless, the finding that previous studies have shown that podocytes may undergo EMT *in vitro*,[52] together with the finding that miRNAs regulate EMT in other cells,[53] suggests that future studies should address whether podocytes undergo EMT *in vivo* and, if so, whether miRNAs play a role in this process.

One of the new findings reported here is that inducible conditional deletion of Drosha in podocytes at 2 months of age led to a rapid CG with proteinuria detected after <2 weeks after being treated with doxycycline. This finding not only supports the critical role for miRNAs in the maintenance of normal function of the mature podocyte, but also strongly supports the idea that primary changes in specific miRNAs in the various podocytopathies may directly mediate disease. Identifying these miRNAs and the genes they regulate will likely provide new insight into disease pathogenesis as well as novel therapeutic targets.

Table 4 | Proliferative index of epithelial cell in urinary space

	Glomeruli with Ki-67+ cells in urinary space per total number of collapsed glomeruli (range)
NPHS2-Cre; Drosha$^{+/+}$	0
NPHS2-Cre; Drosha$^{fl/fl}$ (2 weeks)	0
NPHS2-Cre; Drosha$^{fl/fl}$ (4-6 weeks)	0.656 (0.261–0.753)

MATERIALS AND METHODS

Mice

Podocyte-specific *Drosha* KOs were generated by crossing *NPHS2-Cre* transgenic mice with mice containing a conditional allele of *Drosha*^{fl}. *Drosha*^{fl} contains two *loxP* sites that flank exon 9.[29] *NPHS2-Cre* has been shown to be activated specifically in podocytes using a Rosa26 reporter.[54] Mice were genotyped by PCR using tail DNA and primer pairs as previously reported.[29,54]

Podocyte-specific *Dicer* KOs were generated using a similar strategy by crossing *NPHS2-Cre* transgenic mice with mice containing a conditional allele of *Dicer*^{fl}. *Dicer*^{fl} mice have been previously reported and were a generous gift of M McManus (University of California, San Francisco).[30]

Both *Drosha* and *Dicer* mice were backcrossed onto a C57BL/6 genetic background for eight generations.

Histology

Mice were perfused with 4% paraformaldehyde through the heart. Kidneys were then either embedded in OCT and snap frozen or fixed in 4% paraformaldehyde overnight followed by embedding in paraffin. Periodic acid-Schiff staining was performed on 4 mm paraffin sections according to a standard protocol.[55]

Immunohistochemistry

Paraffin sections were immunostained using the antibodies described below and detected using the avidin-biotin immunoperoxidase technique (Vector Laboratories, Burlingame, CA) or fluorescent antibodies as previously described.[41]

Antibodies

The antibodies used in these studies were: anti-SMA (clone 1A4; Sigma, St Louis, MO), anti-synaptopodin (clone G1D4; Progen Biotechnik, Heidelberg, Germany), anti-WT-1 (Santa Cruz Biotechnology, Santa Cruz, CA), anti-desmin (clone D33; Dako, Carpenteria, CA), anti-nestin (clone 2Q178; Santa Cruz Biotechnology, Santa Cruz, CA), anti-ZO1, Alexa Fluor 594 goat anti-rabbit IgG, and Alexa Fluor 488 goat anti-mouse immunoglobulin (Invitrogen, Carlsbad, CA). Anti-podocin anti-nephrin antibodies are rabbit polyclonal antibodies that have been previously described.

Electron microscopy

Kidney cortex was sliced into 1 mm^3 cubes, fixed in 2% glutaraldehyde solution, and then processed using a standard protocol.

Proteinuria and blood urea nitrogen determination

Urine was collected and protein concentration was determined using the Bradford protein assay (Bio-Rad, Hercules, CA),[56] as well as by the separation of unconcentrated urine by sodium dodecyl

Figure 5 | Pseudocrescents stain positive for desmin, nestin, smooth muscle actin (SMA), and Ki-67. (**a**) Immunohistochemistry of histological sections from 4- to 5-week-old wild-type (WT; *NPHS2-Cre; Drosha*$^{+/+}$), homozygous Drosha (*NPHS2-Cre; Drosha*$^{fl/fl}$), and Dicer (*NPHS2-Cre; Dicer*$^{fl/fl}$) mutants immunostained with antibodies as indicated. (**b**) *NPHS2-Cre; Drosha*$^{fl/fl}$ demonstrate increased apoptosis as collapsing glomerulopathy (CG) becomes more advanced. Statistically significant for 4- and 6-week-old *NPHS2-Cre; Drosha*$^{fl/fl}$ when compared with WT animals or 2-week-old *NPHS2-Cre; Drosha*$^{fl/fl}$ (*$P<0.05$).

sulfate-polyacrylamide gel electrophoresis followed by staining with Coomassie. Blood urea nitrogen concentration on serum was determined using the QuantichromTM urea assay kit (BioAssay Systems, Hayward, CA).

Podocyte proliferation

Paraffin sections (4 mm) were stained with an antibody to Ki-67 (Dako). The PI was determined by counting the number of glomeruli with Ki-67-positive cells in the urinary space per total number of glomeruli as described in Table 4.

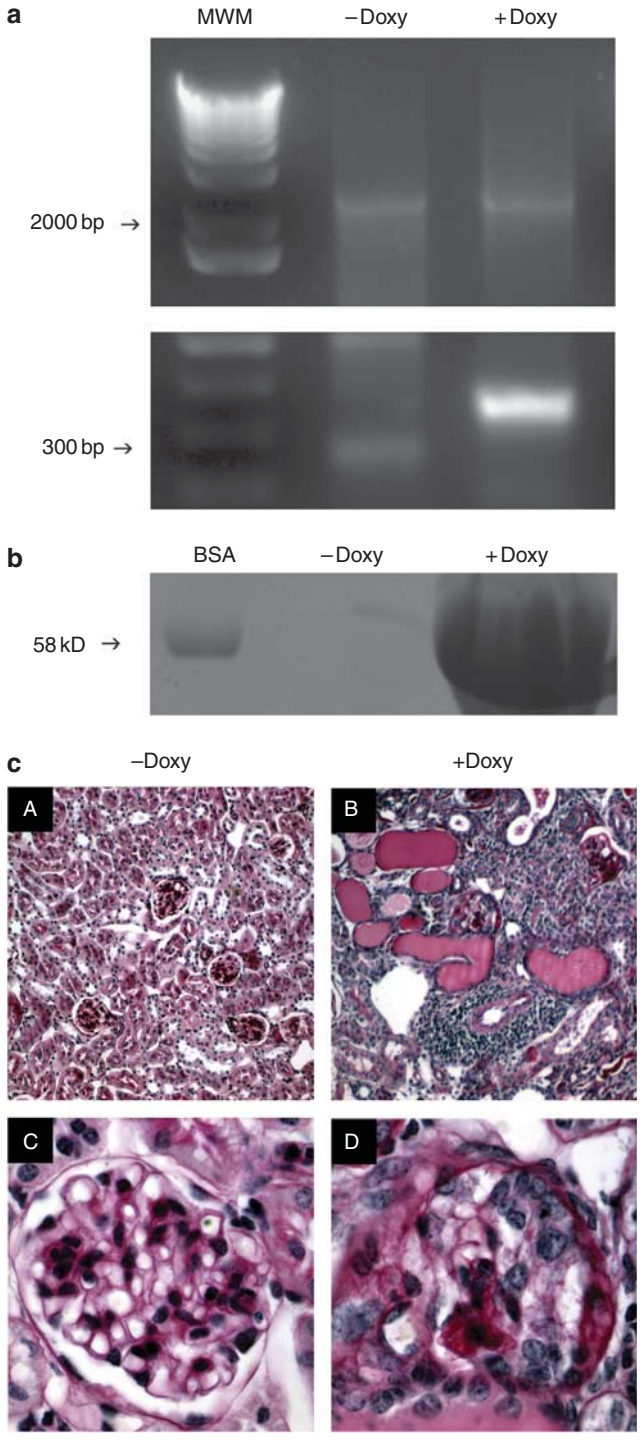

Apoptosis

TUNEL (terminal deoxynucleotidyl transferase dUTP nick end labeling) staining was performed with the DeadEnd Fluorometric TUNEL System as per the manufacturer's directions (Promega, Madison, WI). The number of TUNEL-positive cells per 100 glomeruli was counted in sections from three control and three mutant kidneys from each group.

Generation of conditional inducible deletion of Drosha in podocytes

Drosha$^{fl/fl}$ mice described above were crossed to transgenic mice expressing both the reverse tetracycline transactivator (rtTA) under the control of the podocyte-specific podocin promoter NPHS2 (podocin-rrTA) and the cre recombinase driven by a minimal cytomegalovirus promoter downstream of tet operon sequences. Cre was then induced in 8-week-old mice (*Drosha*$^{fl/fl}$; *podocin-rtTA*$^{Tg/+}$; *tetO-Cre*$^{Tg/+}$) by supplementing doxycyline (4 mg/ml) to the drinking water for 1 to 2 weeks as previously described.[36] Animals were killed 4 weeks after the administration of doxycycline and kidneys were analyzed as described above. *Drosha*$^{fl/fl}$; *podocin-rtTA*$^{Tg/+}$; *tetO-Cre*$^{Tg/+}$ not administered doxycycline served as controls.

Laser capture microdissection and RNA extraction

To isolate glomeruli, laser capture microdissection was performed with PixCell II (Arcturus Bioscience Applied Biosystems by Life Technologies). Frozen kidney sections (4 μm) were dehydrated in graded ethanol solutions, stained with hematoxyin and eosin, placed in xylene, and air dried. Laser capture was performed under direct microscopic visualization by melting of selected regions onto a thermoplastic film mounted on optically transparent LCM caps (Arcturus Engineering, Mountain View, CA). The PixCell II LCM System (Arcturus Engineering) was set to the following parameters: 7.5 μm laser spot size, 60 mW power, and 15.0 ms duration. The thermoplastic film containing the microdissected glomeruli was

Figure 6 | Conditional inducible deletion of Drosha in podocytes in 2-month-old animals results in a collapsing glomerulopathy. (**a**) Glomeruli were isolated from *Drosha*$^{fl/fl}$; *podocin-rtTA*$^{Tg/+}$; *tetO-Cre*$^{Tg/+}$ mice that were either administered or not administered doxycycline and deletion of exon 9 was assessed by PCR using primers that flank the *loxP* site. Deletion of exon 9 results in a product of 334 base pairs, in contrast to the 2.5 Kb product in the wild-type gene. As molecular weight marker (MWM), 1 kB plus Invitrogen was used. (**b**) Urine (10 μl) from *Drosha*$^{fl/fl}$; *podocin-rtTA*$^{Tg/+}$; *tetO-Cre*$^{Tg/+}$ mice that were administered or not administered doxycycline for 2–4 weeks were separated by sodium dodecyl sulfate (SDS)-polyacrylamide gel electrophoreses (10%) followed by Coomassie staining. Bovine serum albumin (BSA) was run as a control. (**c**) *Drosha*$^{fl/fl}$; *podocin-rtTA*$^{Tg/+}$; *tetO-Cre*$^{Tg/+}$ mice were either administered or not administered doxycycline at 2 months of age and kidneys were analyzed 1 month later. Shown are periodic acid-Schiff (PAS) stains of kidneys sections from (A, C) Dox– and (B, D) Dox+ animals. Normal glomeruli and unremarkable tubule–interstitium (×20) is shown in A. On higher magnification (C, ×40), glomeruli are normal in size and cellularity and mesangium is normally expanded. Glomerular basement membranes are also unremarkable. No proliferation in the urinary space is noted. In contrast, animals fed doxycycline (B, ×20) had numerous tubular microcysts and a dense interstitial inflammation, which on higher magnification (D, ×40) revealed shrunken glomeruli, with collapsed capillary walls and proliferation of epithelial cells that filled the urinary space.

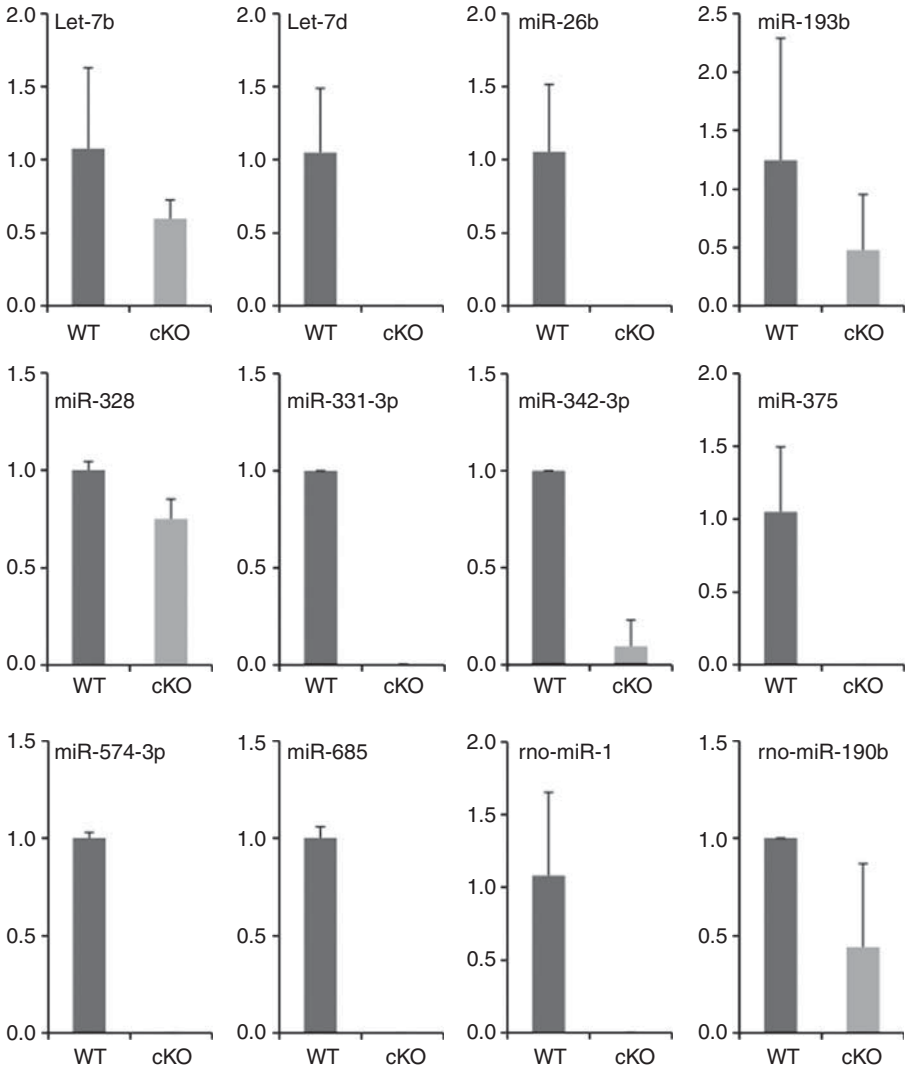

Figure 7 | Micro-RNA (miRNA) expression in glomeruli from Doxycycline– and Doxycyline + animals. The 2-month-old *Drosha*$^{fl/fl}$; *podocin-rtTA*$^{Tg/+}$; *tetO-Cre*$^{Tg/+}$ mice were either administered or not administered doxycycline for 2 weeks and glomeruli were isolated by laser capture microdissection as described in the Materials and Methods section. RNA was then reversed transcribed and miRNA expression was quantitated using Taqman Low Density Microarrays (Applied Biosystems). Shown are 10 miRNAs that were consistently markedly downregulated in doxycycline-treated animals from three independent experiments.

incubated with 50 µl extraction buffer and total RNA was extracted as per the manufacturer's instructions (PicoPure RNA Isolation Ki, KIT0204; Arcturus). To eliminate potential genomic DNA contamination, RNA samples were treated with RNAse-free DNase. RNA concentration was measured by nanodrop and quality assessed by bioanalyzer.

Quantitative-real time PCR profiling on TLDA arrays. Rodent TaqMan Low Density Array (TLDA) plate A and B version 2 microfluidics cards (Applied Biosystems) were used to assess the miRNA profiles. The contents of the TLDA A card comprised a total of 343 miRNAs. Experimental samples from three independent mice were profiled by ABI Prism 7900HT Sequence Detection System and miRNA levels were normalized to the average of U6 and U87 controls contained on the plate. The array data were analyzed by SDS software (Applied Biosystems) using the $RQ = 2.0 - \Delta\Delta CT$ method, visualized in Agilent Genespring GX11 software (Santa Clara, CA) where they were filtered on flag calls, and then analyzed for reproducibly modulated profiles.

Verification of Drosha deletion in podocytes

Glomeruli were isolated from 2-month-old *NPHS2-Cre; Drosha*$^{fl/fl}$ mice that were either untreated or treated with doxycyline for 2 weeks. Glomeruli were then isolated using Dynabeads as previously described,[57] yielding a population of >90% glomeruli. PCR was then performed on glomerular DNA using primers flanking the *loxP* sites (Drosha-F 5′-GCAGAAAGTCTCCCACTCCT-3′, Drosha-R-KO 5′-AACAACTGGGGCTGAAGAGA-3′), which detect deletion of exon 9 in the *Drosha* gene.

DISCLOSURE

All the authors declared no competing interests.

ACKNOWLEDGMENTS

We thank Michael T. McManus for the *Dicer*$^{f/f}$ mice, and Susan Quaggin for the podocin-rtTA;tetO-Cre transgenic mice. We thank the NYU Genome Technology Center supported in part by the NIH/NCI Grant P30 CA016087-30 for expert assistance with TLDA array

profiling of miRNA expression. EYS is supported by Grants R01GM084195 and R01AI052459. OZ is supported in part by grant 1UL1RR029893 from the National Center for Research Resources, National Institutes of Health.

REFERENCES

1. Bartel DP. MicroRNAs: genomics, biogenesis, mechanism, and function. *Cell* 2004; **116**: 281–297.
2. Rana TM. Illuminating the silence: understanding the structure and function of small RNAs. *Nat Rev Mol Cell Biol* 2007; **8**: 23–36.
3. Filipowicz W, Bhattacharyya SN, Sonenberg N. Mechanisms of post-transcriptional regulation by microRNAs: are the answers in sight? *Nat Rev Genet* 2008; **9**: 102–114.
4. Eulalio A, Huntzinger E, Izaurralde E. Getting to the root of miRNA-mediated gene silencing. *Cell* 2008; **132**: 9–14.
5. Lee Y, Ahn C, Han J *et al.* The nuclear RNase III Drosha initiates microRNA processing. *Nature* 2003; **425**: 415–419.
6. Lee Y, Kim M, Han J *et al.* MicroRNA genes are transcribed by RNA polymerase II. *EMBO J* 2004; **23**: 4051–4060.
7. Han J, Lee Y, Yeom KH *et al.* Molecular basis for the recognition of primary microRNAs by the Drosha-DGCR8 complex. *Cell* 2006; **125**: 887–901.
8. Kim VN. MicroRNA biogenesis: coordinated cropping and dicing. *Nat Rev Mol Cell Biol* 2005; **6**: 376–385.
9. Chendrimada TP, Gregory RI, Kumaraswamy E *et al.* TRBP recruits the Dicer complex to Ago2 for microRNA processing and gene silencing. *Nature* 2005; **436**: 740–744.
10. Gregory RI, Chendrimada TP, Cooch N *et al.* Human RISC couples microRNA biogenesis and posttranscriptional gene silencing. *Cell* 2005; **123**: 631–640.
11. Bartel DP. MicroRNAs: target recognition and regulatory functions. *Cell* 2009; **136**: 215–233.
12. Erson AE, Petty EM. MicroRNAs in development and disease. *Clin Genet* 2008; **74**: 296–306.
13. Stefani G, Slack FJ. Small non-coding RNAs in animal development. *Nat Rev Mol Cell Biol* 2008; **9**: 219–230.
14. Garzon R, Calin GA, Croce CM. MicroRNAs in cancer. *Annu Rev Med* 2009; **60**: 167–179.
15. Kato M, Arce L, Natarajan R. MicroRNAs and their role in progressive kidney diseases. *Clin J Am Soc Nephrol* 2009; **4**: 1255–1266.
16. Li JY, Yong TY, Michael MZ *et al.* Review: the role of microRNAs in kidney disease. *Nephrology (Carlton)* 2010; **15**: 599–608.
17. Kato M, Putta S, Wang M *et al.* TGF-beta activates Akt kinase through a microRNA-dependent amplifying circuit targeting PTEN. *Nat Cell Biol* 2009; **11**: 881–889.
18. Wei Q, Bhatt K, He HZ *et al.* Targeted deletion of Dicer from proximal tubules protects against renal ischemia-reperfusion injury. *J Am Soc Nephrol* 2010; **21**: 756–761.
19. Wang Q, Wang Y, Minto AW *et al.* MicroRNA-377 is up-regulated and can lead to increased fibronectin production in diabetic nephropathy. *FASEB J* 2008; **22**: 4126–4135.
20. Krupa A, Jenkins R, Luo DD *et al.* Loss of MicroRNA-192 promotes fibrogenesis in diabetic nephropathy. *J Am Soc Nephrol* 2010; **21**: 438–447.
21. Pandey P, Brors B, Srivastava PK *et al.* Microarray-based approach identifies microRNAs and their target functional patterns in polycystic kidney disease. *BMC Genomics* 2008; **9**: 624.
22. Lee SO, Masyuk T, Splinter P *et al.* MicroRNA15a modulates expression of the cell-cycle regulator Cdc25A and affects hepatic cystogenesis in a rat model of polycystic kidney disease. *J Clin Invest* 2008; **118**: 3714–3724.
23. Anglicheau D, Sharma VK, Ding R *et al.* MicroRNA expression profiles predictive of human renal allograft status. *Proc Natl Acad Sci USA* 2009; **106**: 5330–5335.
24. Shi S, Yu L, Chiu C *et al.* Podocyte-selective deletion of dicer induces proteinuria and glomerulosclerosis. *J Am Soc Nephrol* 2008; **19**: 2159–2169.
25. Ho J, Ng KH, Rosen S *et al.* Podocyte-specific loss of functional microRNAs leads to rapid glomerular and tubular injury. *J Am Soc Nephrol* 2008; **19**: 2069–2075.
26. Harvey SJ, Jarad G, Cunningham J *et al.* Podocyte-specific deletion of dicer alters cytoskeletal dynamics and causes glomerular disease. *J Am Soc Nephrol* 2008; **19**: 2150–2158.
27. Tam OH, Aravin AA, Stein P *et al.* Pseudogene-derived small interfering RNAs regulate gene expression in mouse oocytes. *Nature* 2008; **453**: 534–538.
28. Watanabe T, Totoki Y, Toyoda A *et al.* Endogenous siRNAs from naturally formed dsRNAs regulate transcripts in mouse oocytes. *Nature* 2008; **453**: 539–543.
29. Chong MM, Rasmussen JP, Rudensky AY *et al.* The RNAseIII enzyme Drosha is critical in T cells for preventing lethal inflammatory disease. *J Exp Med* 2008; **205**: 2005–2017.
30. Harfe BD, McManus MT, Mansfield JH *et al.* The RNaseIII enzyme Dicer is required for morphogenesis but not patterning of the vertebrate limb. *Proc Natl Acad Sci USA* 2005; **102**: 10898–10903.
31. DePianto D, Coulombe PA. Intermediate filaments and tissue repair. *Exp Cell Res* 2004; **301**: 68–76.
32. Floege J, Alpers CE, Sage EH *et al.* Markers of complement-dependent and complement-independent glomerular visceral epithelial cell injury in vivo. Expression of antiadhesive proteins and cytoskeletal changes. *Lab Invest* 1992; **67**: 486–497.
33. Floege J, Hackmann B, Kliem V *et al.* Age-related glomerulosclerosis and interstitial fibrosis in Milan normotensive rats: a podocyte disease. *Kidney Int* 1997; **51**: 230–243.
34. Hoshi S, Shu Y, Yoshida F *et al.* Podocyte injury promotes progressive nephropathy in zucker diabetic fatty rats. *Lab Invest* 2002; **82**: 25–35.
35. Thorner PS, Ho M, Eremina V *et al.* Podocytes contribute to the formation of glomerular crescents. *J Am Soc Nephrol* 2008; **19**: 495–502.
36. Jones N, New LA, Fortino MA *et al.* Nck proteins maintain the adult glomerular filtration barrier. *J Am Soc Nephrol* 2009; **20**: 1533–1543.
37. Suh N, Baehner L, Moltzahn F *et al.* MicroRNA function is globally suppressed in mouse oocytes and early embryos. *Curr Biol* 2010; **20**: 271–277.
38. Albaqumi M, Barisoni L. Current views on collapsing glomerulopathy. *J Am Soc Nephrol* 2008; **19**: 1276–1281.
39. D'Agati VD. Podocyte injury in focal segmental glomerulosclerosis: lessons from animal models (a play in five acts). *Kidney Int* 2008; **73**: 399–406.
40. Barisoni L, Schnaper HW, Kopp JB. Advances in the biology and genetics of the podocytopathies: implications for diagnosis and therapy. *Arch Pathol Lab Med* 2009; **133**: 201–216.
41. Barisoni L, Mokrzycki M, Sablay L *et al.* Podocyte cell cycle regulation and proliferation in collapsing glomerulopathies. *Kidney Int* 2000; **58**: 137–143.
42. Appel D, Kershaw DB, Smeets B *et al.* Recruitment of podocytes from glomerular parietal epithelial cells. *J Am Soc Nephrol* 2009; **20**: 333–343.
43. Asano T, Niimura F, Pastan I *et al.* Permanent genetic tagging of podocytes: fate of injured podocytes in a mouse model of glomerular sclerosis. *J Am Soc Nephrol* 2005; **16**: 2257–2262.
44. Dijkman HB, Weening JJ, Smeets B *et al.* Proliferating cells in HIV and pamidronate-associated collapsing focal segmental glomerulosclerosis are parietal epithelial cells. *Kidney Int* 2006; **70**: 338–344.
45. Moeller MJ, Soofi A, Hartmann I *et al.* Podocytes populate cellular crescents in a murine model of inflammatory glomerulonephritis. *J Am Soc Nephrol* 2004; **15**: 61–67.
46. Suzuki T, Matsusaka T, Nakayama M *et al.* Genetic podocyte lineage reveals progressive podocytopenia with parietal cell hyperplasia in a murine model of cellular/collapsing focal segmental glomerulosclerosis. *Am J Pathol* 2009; **174**: 1675–1682.
47. Smeets B, Uhlig S, Fuss A *et al.* Tracing the origin of glomerular extracapillary lesions from parietal epithelial cells. *J Am Soc Nephrol* 2009; **20**: 2604–2615.
48. Kim HK, Lee YS, Sivaprasad U *et al.* Muscle-specific microRNA miR-206 promotes muscle differentiation. *J Cell Biol* 2006; **174**: 677–687.
49. Chen JF, Callis TE, Wang DZ. microRNAs and muscle disorders. *J Cell Sci* 2009; **122**: 13–20.
50. Zeisberg M, Neilson EG. Biomarkers for epithelial-mesenchymal transitions. *J Clin Invest* 2009; **119**: 1429–1437.
51. Kalluri R, Weinberg RA. The basics of epithelial-mesenchymal transition. *J Clin Invest* 2009; **119**: 1420–1428.
52. Li Y, Kang YS, Dai C *et al.* Epithelial-to-mesenchymal transition is a potential pathway leading to podocyte dysfunction and proteinuria. *Am J Pathol* 2008; **172**: 299–308.
53. Korpal M, Kang Y. The emerging role of miR-200 family of microRNAs in epithelial-mesenchymal transition and cancer metastasis. *RNA Biol* 2008; **5**: 115–119.
54. Moeller MJ, Sanden SK, Soofi A *et al.* Podocyte-specific expression of cre recombinase in transgenic mice. *Genesis* 2003; **35**: 39–42.
55. Barisoni L, Bruggeman LA, Mundel P *et al.* HIV-1 induces renal epithelial dedifferentiation in a transgenic model of HIV-associated nephropathy. *Kidney Int* 2000; **58**: 173–181.
56. Bradford MM. A rapid and sensitive method for the quantitation of microgram quantities of protein utilizing the principle of protein-dye binding. *Anal Biochem* 1976; **72**: 248–254.
57. Takemoto M, Asker N, Gerhardt H *et al.* A new method for large scale isolation of kidney glomeruli from mice. *Am J Pathol* 2002; **161**: 799–805.